JOURNAL OF GEOPHYSICAL RESEARCH, VOL. 88, NO. A4, PAGES 3046–3054, APRIL 1, 1983

A Source of the Backstreaming Ion Beams in the Foreshock Region

MOTOHIKO TANAKA

Institute for Physical Science and Technology, University of Maryland, College Park, Maryland 20742

C. C. GOODRICH, D. WINSKE, AND K. PAPADOPOULOS

Department of Physics and Astronomy, University of Maryland, College Park, Maryland 20742

A new source mechanism is proposed for the 'reflected' ion beams observed in the foreshock region of the earth's bow shock. In our model the beams originate in the magnetosheath downstream of the quasi-perpendicular portion of the shock. The quasi-perpendicular shock transition is characterized by two downstream ion populations including high-energy gyrating ions in addition to the directly transmitted anisotropic ions. We show by particle simulations that this highly anisotropic downstream ion distribution ($T_\perp/T_\parallel \gg 1$) can excite electromagnetic ion cyclotron waves which, in turn, pitch angle scatter the gyrating ions in a few ion gyroperiods. As a result, some ions acquire large parallel velocities and move fast enough along the convecting downstream magnetic field to escape back across the bow shock into the upstream region. The distribution of escaping ions calculated by using the pitch-angle-scattered ions, as a source, becomes a beam with a large temperature anisotropy $T_\perp \sim 3$–$5\ T_\parallel$ and a mean velocity along the magnetic field of about twice that of the solar wind velocity. A significant result is the presence of the maximum angle $\theta_{nB} = \theta_c$ above which no ions can escape, where θ_{nB} is the angle between the shock normal and the interplanetary magnetic field. A wide peak of constant escaping ion flux is formed below θ_c whose number density is 1–2% of that of the solar wind. These results are in general agreement with the ISEE observations of the 'reflected' ions.

1. INTRODUCTION

A prominent and well-known feature of the earth's bow shock is the presence of backstreaming ions upstream from the bow shock [*Asbridge et al.*, 1968; *Lin et al.*, 1974]. The morphology of these upstream ions has been clarified in recent years by the accumulation of observational results [*Gosling et al.*, 1978; *Bame et al.*, 1980; *Greenstadt et al.*, 1980; *Paschmann et al.*, 1981; *Bonifazi and Moreno*, 1981*a*, *b*]. Figure 1 shows the basic geometry in the ecliptic plane. The solar wind (arrows) and convected magnetic field (straight lines, oriented at an angle $\sim 45°$ with respect to the solar wind) intersect the magnetosphere at the bow shock (curved surface); the magnetic field and the shock normal intersect at an angle θ_{nB}, which varies along the shock front. Shown as inserts in the figure are the two basically different, spatially separated populations of backstreaming ions (figures from *Paschmann et al.* [1981]). The 'reflected' ions are well-collimated beams of ions with energies of a few keV backstreaming along the interplanetary magnetic field from the bow shock. They appear to emanate from a region of the shock having θ_{nB}, primarily between 70° and 30° (above the dashed line in Figure 1), that is, the quasi-perpendicular shock. The 'diffuse' ions are a roughly isotropic, hot (~ 30 keV) ion population. These ions are commonly observed for $\theta_{nB} \lesssim 45°$ (below the dashed line), the quasi-parallel shock. Between these regions a smooth change of the ion populations from beamlike to isotropic is observed. This transition population is called 'intermediate' ions. At present, the source mechanism for neither population is well understood.

We are concerned here with the source of the 'reflected' ion beams. Although the observations are not yet sufficient to elicit the source mechanism, the well-documented characteristics of the 'reflected' ion beams constitute a stringent test for any proposed mechanism. The bulk of the ion beams are observed for $\theta_{nB} \lesssim 70°$. Their characteristics (for $\theta_{nB} < 70°$) appear to be roughly independent of θ_{nB} [*Paschmann et al.*, 1981; *Bonifazi and Moreno*, 1981*a*, *b*]. On the average, the beam flow speed along the magnetic field is twice as large as the solar wind speed V_{sw}, though it can be sometimes significantly higher. The density of the beam averages about 1% of that of the solar wind. The beams are consistently anisotropic with $T_\perp/T_\parallel \sim 2$–$3$ [*Paschmann et al.*, 1981], where $T_\perp$ ($T_\parallel$) is the temperature perpendicular (parallel) to the magnetic field. The magnitude of $T_\perp$ is much larger than the solar wind temperature ($T_{i,sw} \sim 5$ eV); in fact, $T_\perp \sim 0.1$–1 keV. For $\theta_{nB} > 70°$, more energetic beams are observed with speeds a factor of 5 or more larger than V_{sw}. These beams also have consistently large temperature and thermal anisotropy.

It has been commonly suggested [*Greenstadt*, 1975; *Gosling et al.*, 1978; *Bame et al.*, 1980; *Bonifazi and Moreno*, 1981*a*, *b*] that these ions are a small part of the solar wind ions which are reflected near the quasi-perpendicular portion of the bow shock; hence the name 'reflected' ions, primarily due to their collimated nature and apparent geometric origin. The major evidence supporting reflection as the source of these ions results from studies of the resulting ion energy gain [*Sonnerup*, 1969; *Greenstadt*, 1975; *Paschmann et al.*, 1980]. *Sonnerup* [1969] has shown using conservation laws that ions can be accelerated by their displacement along the interplanetary motional electric field during their reflection at the shock. His results, which have been extended to a more general shock geometry by *Paschmann et al.* [1980], relate the energy gain of an ion during reflection to θ_{nB} and the change in the direction of the ion trajectory. The maximum energy gain is obtained when the ion magnetic moment is conserved during reflection; for large θ_{nB} the energy gain is proportional to $\tan^2 \theta_{nB}$ and can be quite large. *Paschmann et al.* [1980] analyzed a number of ISEE upstream ion events and found that the geometric energization formulas assuming μ is conserved generally agree with the observed ion beam streaming energies.

Paper number 3A0174.
0148-0227/83/003A-0174$05.00

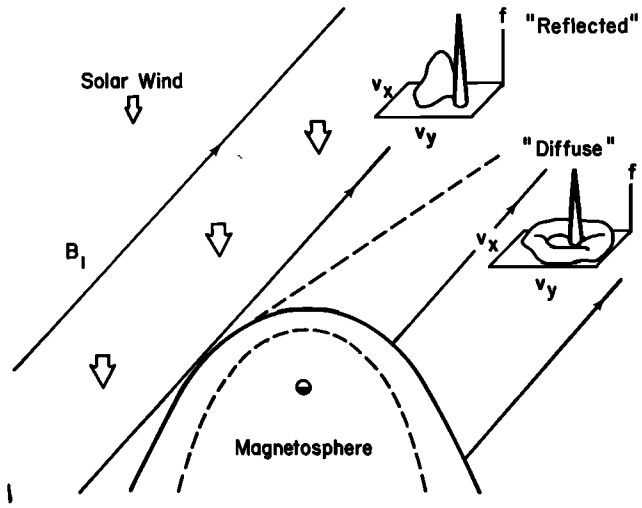

Fig. 1. Basic geometry of the earth's bow shock. Sketches at the top right corner show the location and shape of two ion distributions; sharp peaks correspond to the solar wind and the other to backstreaming ions in the foreshock region.

The case for direct reflection as the ion beam source is not compelling, however. Observationally, there is evidence that at least a substantial fraction of the ions are not geometrically accelerated. In a statistical analysis of ion events observed at ISEE 2, *Bonifazi and Moreno* [1981*a*, *b*] found the average ion beam speed to be approximately constant at twice the solar wind speed for $35° \lesssim \theta_{nB} \lesssim 70°$. These results are significantly below the beam speeds predicted by the formulas of *Sonnerup* [1969] and *Paschmann et al.* [1980], assuming that μ is conserved, and would appear to contradict the findings of *Paschmann et al.* [1980]. However, there is considerable scatter in the *Paschmann et al.* [1980] data for the events with $\theta_{nB} < 70°$ with most of the beam speeds below the predicted values. In fact, for $35° \lesssim \theta_{nB} \lesssim 65°$, while they also report significantly faster ion beams, a substantial number of the ion events in the work of *Paschmann et al.* [1980] are consistent with the *Bonifazi and Moreno* [1981*a*, *b*] results. Further, it is difficult to explain the large temperatures of the upstream ion beam observed in the context of direct reflection, since if μ is conserved, the beam temperature would be approximately the solar wind temperature. If μ is assumed to increase during reflection, then the ion perpendicular temperature could be increased significantly. Since this gain comes at the expense of the streaming energy, deviations in μ could in principle explain the observed scatter in the upstream ion beam speeds. However, in this case, there should be an inverse correlation between beam temperature and speed (at fixed θ_{nB}). The observed beam parallel temperatures cannot be explained in this way, as it is quite insensitive to changes in μ.

A weakness of the direct reflection model is that no reasonable reflection mechanism has been proposed that conserves, or approximately conserves, μ. In fact, for the quasi-perpendicular bow shock ($\theta_{nB} \gtrsim 45°$), such a mechanism is theoretically difficult to justify. It is well established observationally (J. D. Scudder et al., unpublished manuscript, 1982) and theoretically [*Tidman and Krall*, 1971; *Wu*, 1982] that the major magnetic field jump has a scale much shorter than the ion gyroradius. In fact, observational [*Paschmann et al.*, 1982] and numerical simulation [*Leroy et al.*, 1981, 1982] studies of ion reflection at the quasi-perpendicular bow shock show that μ is far from constant. They find that reflection is instead specular and that reflected ions do not receive the large energy gain assumed in the work of *Paschmann et al.* [1980]. Moreover, the magnetic mirror force [e.g., *Terasawa*, 1979], which has been suggested as an ion reflection mechanism and could be expected to conserve μ, cannot reflect solar wind thermal ions. Typically 99.9% of the solar wind ions have pitch angles less than 15°, whereas the pitch angle must be greater than ~30° for mirror reflection.

Thus it is important to consider sources other than direct reflection for the upstream ion beams. One possible source is leakage upstream of hot magnetosheath ions. Recently, *Edmiston et al.* [1982] considered this approach in an idealized model in which the ions are heated and thermalized in a thin layer at the shock front. They calculated the ions returning upstream from a hot Maxwellian distribution at this layer. Within their model, which does not address the actual heating mechanism, significant upstream ion fluxes occur only for the quasi-parallel portion ($\theta_{nB} \lesssim 45°$) of the bow shock. Their results thus appear to be relevant to the diffuse rather than the 'reflected' ions.

In this paper we propose a new and self-consistent source mechanism for the 'reflected' ions based on the observed [*Paschmann et al.*, 1982] and theoretically understood [*Leroy et al.*, 1981, 1982] ion behavior in the quasi-perpendicular shock. As the work of *Edmiston et al.* [1982], the ion source is in the magnetosheath. The process is summarized in Figure 2. The solar wind, when it encounters the quasi-perpendicular portion of the earth's bow shock, is adiabatically compressed and heated in the perpendicular direction and transmitted into the magnetosheath (called 'core ions' hereafter). At the same time, some of the solar wind ions are reflected at the shock front through a combination of magnetic and electrostatic forces and gain energy due to their Larmor displacement in the direction of the $\mathbf{E} = \mathbf{V}_{sw} \times \mathbf{B}_1$ electric field. These ions, however, are all magnetically deflected back through the shock front (called 'gyrating ions') [*Leroy et al.*, 1981, 1982]. These two distinct types of ions at the quasi-perpendicular shock have recently been observed [*Montgomery et al.*, 1970; *Paschmann et al.*, 1982]. Both kinds of ions thus acquire large perpendicular

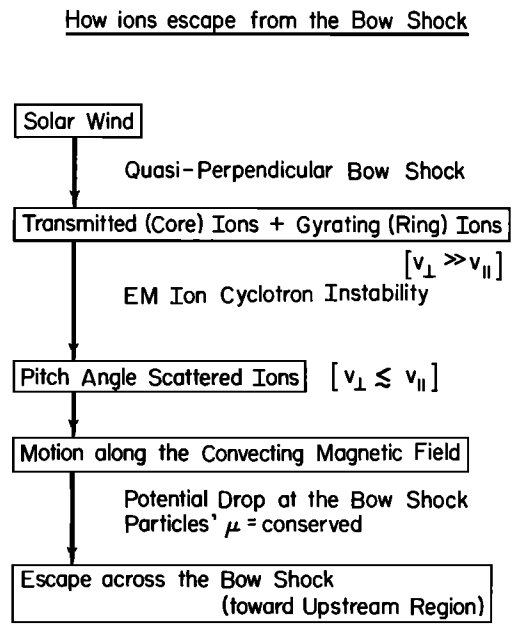

Fig. 2. Flow chart of the proposed ion reflection process.

energies compared with their parallel energies. The free energy associated with this anisotropy then drives the electromagnetic ion cyclotron (EMIC) instability. As the result of the instability, the gyrating ions are pitch angle scattered, producing some ions with large parallel velocities. These ions then move along the convecting magnetic field lines, cross the bow shock, and escape into the upstream region.

In section 2 of this paper, it will be shown by particle simulations that the gyrating ions created at the quasi-perpendicular bow shock are effectively scattered by the EMIC instability. Using the ion distribution resulting from this process, we calculate the flux and distribution functions of ions escaping upstream in section 3. Finally, section 4 is devoted to a discussion and summary of the results.

2. Ion Scattering Mechanism—Particle Simulations of EMIC Waves

The results of the hybrid simulations [*Leroy et al.*, 1981, 1982] show that there are two types of ions behind the quasi-perpendicular bow shock. Figure 3 shows the velocity distribution of ions (x corresponds to the shock normal direction) perpendicular to the magnetic field just behind the shock front computed in the simulation. (The parameters were chosen to emulate the ISEE shock crossing of November 7, 1977; for a detailed description of the hybrid model and results, see *Leroy et al.* [1981].) Most of the ions ($\gtrsim$ 85%) are slowed and adiabatically heated in the perpendicular direction (their perpendicular temperature becomes roughly 4–8 times greater than their parallel temperature) as they traverse the shock transition layer to form an anisotropic ion 'core.' Surrounding these 'core' ions is a diffuse ring of more energetic ions. These ions were initially reflected at the shock front and then magnetically deflected downstream. Their gyrating orbits and phase mixing cause them to be spread out roughly in a ring in velocity space. Typically the perpendicular energy of these 'ring' ions is 3 to 4 times larger than their bulk flow energy before encountering the bow shock. This configuration contains a large amount of free energy, due to the large differences in the perpendicular and parallel energies of both the 'ring' and 'core' ions and also to the loss cone nature of the perpendicular velocity distribution of the ring ions, which can drive various instabilities, the most important of which is the electromagnetic ion cyclotron instability [*Davidson and Ogden*, 1975; *Tajima et al.*, 1977; *Lee et al.*, 1981]. Although this instability has been studied previously, the presence of the energetic ring changes its characteristics significantly. In particular, the eventual saturated nonlinear state of the instability is of interest here. In order to investigate the nonlinear behavior, we have performed one-dimensional particle simulations using a finite-size particle magnetostatic code, in which the transverse component of the radiation term is neglected in Maxwell equations [*Busnardo-Neto et al.*, 1977].

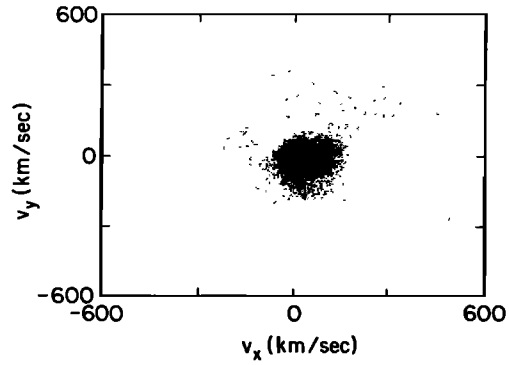

Fig. 3. Velocity distribution of ions in the downstream region of the perpendicular bow shock [*Leroy et al.*, 1982]. The magnetic field is perpendicular to the page.

For the initial state we use three species: isotropic electrons, anisotropic core ions with the perpendicular temperature $T_\perp{}^c$ greater than the parallel temperature $T_\parallel{}^c$, and gyrating ions which have a ringlike velocity distribution and thus have large perpendicular velocities. Then, the average temperature anisotropy $\langle T_\perp\rangle/\langle T_\parallel\rangle = \frac{1}{2}\langle v_y{}^2 + v_z{}^2\rangle/\langle v_x{}^2\rangle \sim \frac{1}{2}(\varepsilon v_0{}^2 + 2\varepsilon' v_{\perp c}{}^2)/(\varepsilon v_{\parallel r}{}^2 + \varepsilon' v_{\parallel c}{}^2)$ is much larger than unity. Here v_0 is the gyrating speed of the ring ions; $v_\perp$ ($v_\parallel$) is the perpendicular (parallel) ion thermal speed. The subscripts c and r denote core and ring, respectively, and $\varepsilon = n_r/(n_r + n_c)$ is the ratio of ring ion density to total ion density, $\varepsilon' = 1 - \varepsilon$. There is an ambient magnetic field pointing in the x direction, and all physical quantities are assumed periodic in this direction within the system of size $L = 16c/\omega_{pi} = 128$ cells, where c/ω_{pi} is the ion inertia length. Particles (electrons and ions) are allowed to move in only one dimension (x) spatially, but all three velocity and field components are kept. We use the following parameters for the initial conditions: the ratio of electron cyclotron frequency to electron plasma frequency $\omega_{ce}/\omega_{pe} = 0.5$, the ratio of electron thermal speed to the speed of light $v_{te}/c = 0.14$, and the mass ratio of ions to electrons $m_i/m_e = 25$. The 6400 ions and 6400 electrons with finite sizes used in the simulation are sufficient to insure that collisions are insignificant on the time scale of the simulation. As usual, the cell size (which corresponds to the particle size) is roughly an electron Debye length.

Results of two runs (A and B) for which the initial perpendicular energy is the same, but distributed between the core and ring ions differently, are presented. For each case the density ratio $\varepsilon = n_r/(n_r + n_c)$ is chosen to be 0.1 (compare hybrid simulations by *Leroy et al.* [1981, 1982]), and the average temperature anisotropy at $t = 0$ is $\langle T_\perp\rangle/\langle T_\parallel\rangle \sim 12$. The difference between run A and run B is the different gyrating velocity of ring ions. It is represented in terms of the effective temperature $T_{\perp r} = \frac{1}{2}m_i v_{\perp r}{}^2 \sim 80T_{\parallel c}$ and $40T_{\parallel c}$ for run A and run B, respectively, where $T_{\parallel c} = \frac{1}{2}m_i v_{\parallel i}{}^2$ is the parallel temperature of core ions. For run A, two thirds of the ion energy is contained in the ring ions, while for run B, only one third of the perpendicular ion energy is in the ring.

The temporal development of Fourier amplitudes of the perturbed magnetic field $|B_z(k, t)|$ for run A is shown in Figure 4. Waves grow in time to $\omega_{ci}\, t \sim 15$ and saturate ($\omega_{ci} = eB/m_i c$ is ion cyclotron frequency). Mode 4 with $ck/\omega_{pi} \sim 1.6$ is the most dominant mode during the early stage of the instability. After $\omega_{ci}\, t > 15$, the longer-wavelength mode $n = 2$ dominates, in accordance with decrease in temperature anisotropy [*Davidson and Ogden*, 1975]. The oscillations of each Fourier mode are due to the existence of both left and right propagating waves. The frequency of the waves can be determined from these oscillations by assuming that the amplitudes of the right and left traveling waves are equal, yielding

$$B_k(t) = 2B_0 \sin kx \cos \omega_r t$$

Therefore $|B_k(t)|$ oscillates in time with period $\Delta t = \pi/\omega_r$, where ω_r is the frequency. The growth rate is calculated from the growth of the upper envelope of $B_k(t)$. Linear characteristics of the waves obtained in this manner (to a measurement accuracy of about 20%) for run A (solid circles) and B (open circles) are

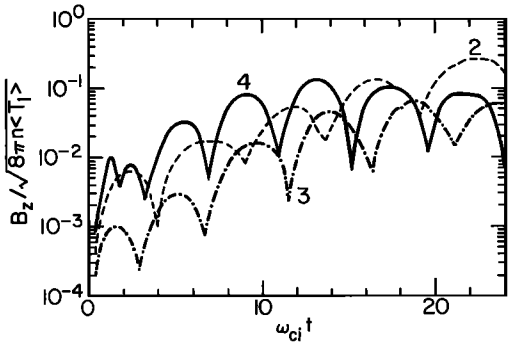

Fig. 4. Temporal development of Fourier amplitudes for run A for various mode numbers. The perturbed field B_z is normalized by the square root of the initial ion energy density, where $\langle T_i\rangle = \frac{1}{2}T_{i\parallel} + T_{i\perp}$.

shown in Figure 5. The solid lines in the figure are the theoretical results obtained from the linear dispersion relation of the electromagnetic ion cyclotron instability for the same parameters [*Davidson and Ogden*, 1975]. This dispersion relation is given by

$$D^{\pm}(\omega, k) = \omega^2 - c^2k^2 + \omega_{pe}{}^2 \frac{\omega}{kv_e} Z(\xi_e{}^{\pm}) + \omega_{pi}{}^2 \frac{\omega}{kv_{i\parallel}} Z(\xi_i{}^{\pm}) - \omega_{pi}{}^2(1 - T_{i\perp}/T_{i\parallel})[1 + \xi_i{}^{\pm}Z(\xi_i{}^{\pm})] = 0$$

where $\xi_e{}^{\pm} = (\omega \mp \omega_{ce})/kv_e$, $\xi_i{}^{\pm} = (\omega \mp \omega_{ci})/kv_{i\parallel}$, $v_e = (2T_e/m_e)^{1/2}$, $v_{i\parallel} = (2T_{i\parallel}/m_i)^{1/2}$, $Z(\xi)$ is the plasma dispersion function, and the ion perpendicular temperature is

$$T_{i\perp} = 2\pi \int_0^{\infty} dv_\perp v_\perp (m_i v_\perp{}^2/2) G(v_\perp)$$

where the ion distribution function $f_i = (\pi v_{i\parallel}{}^2)^{-1/2} G(v_\perp) \exp(-v_\parallel{}^2/v_{i\parallel}{}^2)$ is assumed. The ion perpendicular temperature appears only once through $(1 - T_{i\perp}/T_{i\parallel})$ and is independent of the form of G. In the limit of $T_{i\perp}/T_{i\parallel} \to \infty$, the frequency and the growth rate are $\omega \sim \mp \omega_{ci}$, $\gamma \lesssim (\beta_{i\perp}/2)^{1/2}\omega_{ci}$. The growth rate is an increasing function of the anisotropy $T_{i\perp}/T_{i\parallel}$ and the ion beta $\beta_{i\perp}$. Because both runs have the same total perpendicular energy, the linear properties of runs A and B are expected to be the same. This is verified in the figure. In addition, the frequency and growth rate of the individual modes (2, 3, 4) agree well with the theory.

The relaxation of the ion temperature anisotropy is shown in Figure 6. After a time $\omega_{ci}t \gtrsim 8$, when the magnetic field fluctuations $\langle \delta B^2\rangle$ become large enough, $\langle \delta B^2\rangle/8\pi n\langle T_i\rangle \gtrsim 10^{-3}$, the ion temperature anisotropy starts decreasing. ($\langle T_i\rangle = \langle T_{i\perp} + \frac{1}{2}T_{i\parallel}\rangle$ is the average energy of all the ions.) In each run the anisotropy decreases at roughly the same rate to nearly the same final value of $T_\perp/T_\parallel \sim 3$. The magnetic field fluctuations shown in Figure 6 as an increasing line in run A stop growing at the same time when the anisotropy reaches its minimum value. The level of the fluctuations of saturation $\langle \delta B^2\rangle/8\pi n\langle T_i\rangle$ is about 0.04 in each case. We expect these results to be valid for the bow shock in spite of the unrealistically small mass ratio $m_i/m_e = 25$ used in the simulations. For $\omega_{ci}{}^2/\omega_{pi}{}^2 \ll 1$ and $\beta_e \sim 1$, the dispersion and quasi-linear equations scale as ck/ω_{pi}, ω/ω_{ci}, and ε_k/nT_{i0}, where $\varepsilon_k = |E_k|^2/8\pi$ is the spectral energy density. These scaled equations contain only two parameters $T_{i\perp}/T_{i\parallel}$ and $\beta_{i\parallel}$ and do not include m_i/m_e [cf. *Davidson and Ogden*, 1975].

Changes in the ion distribution due to the EMIC instability are clearly manifested in the $(v_\parallel, v_\perp)$ space plots of Figure 7 for run A. The electron distribution remains Maxwellian and is heated very little (consequently not shown here). The core ions are heated in the parallel direction (reducing the anisotropy from 4.6 to 2.6 for run A), but they stay approximately bi-Maxwellian even at $\omega_{ci}t \sim 36$ of run A. On the other hand, the ring ion distribution changes significantly. Ring ions, initially at $(v_\parallel, v_\perp) = (0, v_0) = (0., 0.25)$ in the simulation, are ptich angle scattered along paths of constant energy $v_\perp{}^2 + (v_\parallel - v_\phi)^2 =$ const, where $v_\phi = \pm|\omega/k|$ is the wave phase velocity; this type of particle scattering was theoretically studied previously [*Kennel and Engelmann*, 1966]. Thus some of the ring ions eventually gain a parallel velocity $v_\parallel \sim v_0 - |v_\phi|$ and the ion distribution function $f(v_\parallel, v_\perp)$ approaches a constant value along these paths. As shown in Figure 7, such a state is nearly achieved at $\omega_{ci}t = 24$, when the fluctuating magnetic field energy saturates. It should be noted that these constant density distributions are realized in a finite length of time, say in a few gyroperiods. (Note that the particle density in Figure 7 shows $fd^3v = 2\pi f v_\perp dv_\parallel dv_\perp$; therefore there are few particles near the $v_\parallel$ axis.)

The one-dimensional nature of the simulation restricts wave vectors to being parallel to the ambient magnetic field. Thus instabilities which involve the interaction of the ring ions with either the electrons or the core ions [*Kulygin et al.*, 1971; *Lee and Birdsall*, 1979*a*, *b*] are excluded. The former instability primarily leads to modification of the electrons, and that is not

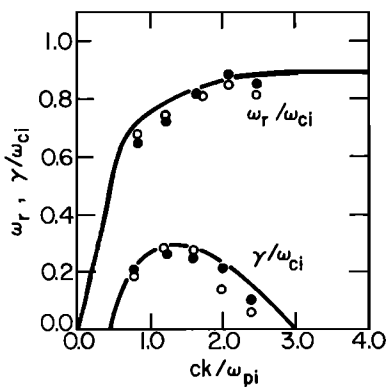

Fig. 5. Linear frequencies and growth rates for the electromagnetic ion cyclotron instability; solid (open) circles correspond to run A (run B), and solid curves are theoretical values [*Davidson and Ogden*, 1975].

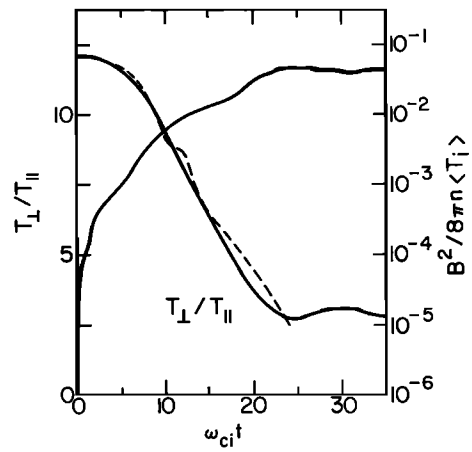

Fig. 6. Relaxation of the temperature anisotropy. Solid (dashed) lines correspond to run A (run B). The total wave energy for run A is shown as an increasing line.

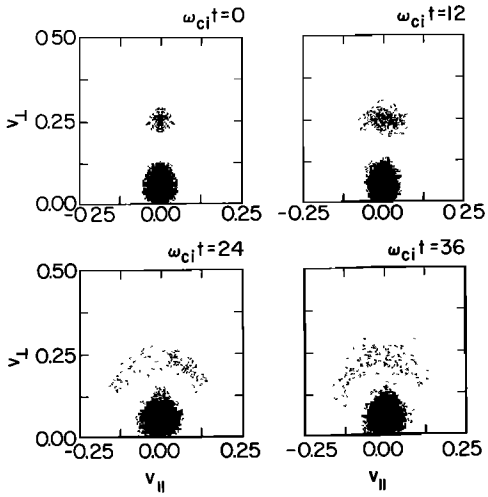

Fig. 7. Plots of the ion velocity distributions in ($v_{\parallel}$, $v_{\perp}$) space at various times for run A.

of interest here. The latter, however, leads to an increased thermal spread of the ring with some of the ions scattered to slightly higher energies. Finally, the simulations implicitly assume that the ion distributions are initially gyrotropic. In fact, the actual distributions may have some angular dependence, which could give rise to obliquely propagating modes. However, the principal instability is the one considered here, which is insensitive to the exact form of the perpendicular velocity distribution.

3. Upstream Ion Distributions

The pitch angle scattering by EMIC waves of the 'ring' ions produces ions with larger $v_{\parallel}$. These ions can escape upstream by moving along a field line which, owing to the curvature of the bow shock, crosses the shock surface. Due to the convection of the plasma during the finite scattering time τ_s, the isotropization occurs a distance $d \sim u_2\tau_s$ downstream of the shock, where u_2 is the downstream normal velocity. It was shown in section 2 that $\tau_s \simeq 20\omega_{ci}^{-1}$, so that $d \simeq 20u_2/\omega_{ci}$; for typical downstream parameters $\omega_{ci} \simeq 2s^{-1}$, $u_2 \simeq 100$ km/s, which implies $d \simeq 1000$ km. The parallel velocity of the scattered ions is roughly v_0, where v_0 is the gyration velocity of the 'ring' ions and is large in comparison with u_2. *Leroy et al.* [1982] have shown v_0 to be about twice the incident velocity normal to the shock, independent of Mach number and ion temperature. By following the trajectories of the scattered ions, the properties of resulting upstream ion population can be determined. Since our model is based on the properties of the quasi-perpendicular portion of the bow shock surface (i.e., $\theta_{nB} \gtrsim 45°$), we expect our results to be valid for $\theta_{nB} \gtrsim 45°$ and progressively less accurate for smaller θ_{nB}. For angles $\theta_{nB} \lesssim 45°$, the gyrating ions do not necessarily reenter the shock [*Gosling et al.*, 1982], so our ion source model becomes increasingly doubtful. We further restrict our attention to the ecliptic plane for convenience only; the results generally are valid.

The physical model used in our calculations, which are carried out in the shock frame, is illustrated in Figure 8. The solar wind flow is assumed to be radial (the earth is at the origin). The interplanetary field at the bow shock B_1, unless otherwise specified, is taken to be along the average Parker spiral, that is, in the ecliptic plane inclined by 45° from the sun-earth line. The bow shock surface is taken to be a circular arc (solid arc in Figure 8) of radius $R = 25\,R_E$. The downstream flow velocity u_2 and density n_2 are determined locally using the Rankine-Hugoniot relations. We assume an isotropized ion source located a distance $d = u_2\tau_s$ behind the shock surface (dashed arc). The scattered ion source extends along the entire shock front, but the density of the scattered ions is assumed to be a maximum at $\theta_{nB} = 90°$ and decreases as $\sin^2\theta_{nB}$ (sensitivity to this assumption is discussed later in this section). Consistent with the results of section 2, the velocity space density of scattered ions is constant on surfaces of $v_{\perp}^2 + (v_{\parallel} - \omega/k - u_{\parallel})^2 = \text{const} = v_0^2 + \omega^2/k^2$, where $u_{\parallel}$ is the parallel downstream bulk velocity and ω/k is the EMIC wave phase speed. (X_0, X_1, and X_2 in Figure 8 will be explained later.)

Since the scattered ions basically move along the field lines, the global orientation of the downstream field is important to the model. As limiting cases we have first considered the field to be determined locally in accordance with the Rankine-Hugoniot relations (model A) and second to be parallel to the upstream field (model B), which is valid for $\theta_{nB} = 90°$ and (over) emphasizes the global nature of the field. However, we will discuss primarily the results for an intermediate case (model C) in which the field is taken to be the average of the above extremes.

In determining the passage of ions across the shock surface itself, it is necessary to consider the structure of the transition layer, in particular, the electrostatic potential. We assume an asymptotic potential jump $e\phi_2$ of $1/4\ m_i V_{sw}^2$; the upstream potential is $e\phi_1$, which is taken to be zero. Within the transition layer, however, we assume significant potential overshoot $\phi_{max} > \phi_2$ [*Leroy et al.*, 1981]. The value of ϕ_{max} is roughly $\frac{3}{2}\phi_2$ for $\theta_{nB} = 90°$, and its overshoot is assumed to decrease as $\sin^2\theta_{nB}$. The overshoot blocks the escape of some of the ions, particularly for moderate θ_{nB}. It is also assumed that the magnetic moment of the ions is constant in crossing the layer. The upstream parameters used in this calculation correspond to the ISEE shock crossing of November 7, 1977 (J. D. Scudder et al., unpublished manuscript, 1982). The Alfven Mach number is $M_A = 8$ at $\theta_{nB} = 90°$, ion and electron beta are $\beta_i = 0.9$ and $\beta_e = 2.2$, plasma density is $n_1 = 12\ \text{cm}^{-3}$, and the magnetic field is 5 γ. The corresponding solar wind velocity is about 360 km/s, and density n_2 and the magnetic field B_2 just behind the perpendicular shock are $n_2 = 40.4\ \text{cm}^{-3}$ and $B_2 = 16.8\ \gamma$.

The velocity space distributions of ions which escape into the foreshock region, calculated using model C, are shown in

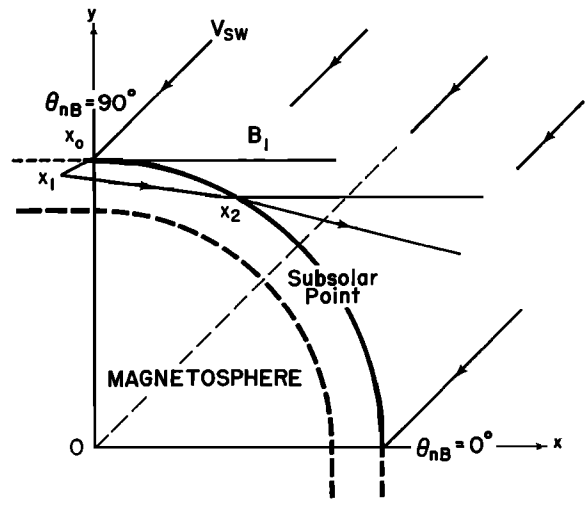

Fig. 8. Geometry and coordinate system for the escaping ion calculation.

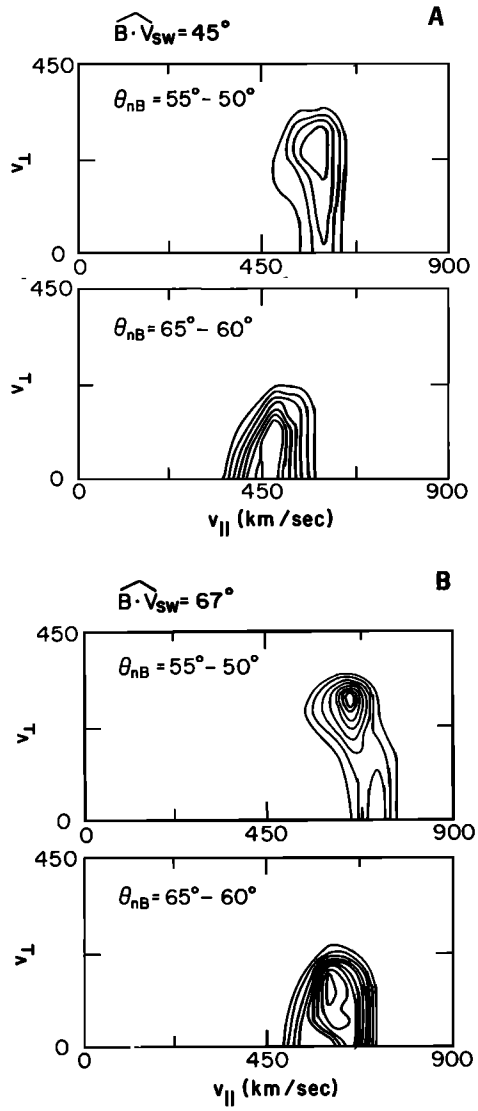

Fig. 9. Equal density contours of escaping ions in the $(v_{\parallel}, v_{\perp})$ velocity space in the shock rest frame for θ_{nB} in the range 50°–55° and 60°–65°. The solar wind and the interplanetary magnetic field are assumed to form an angle of (*a*) 45° and (*b*) 67°, and the solar wind velocity is 360 km/s. The upstream bulk speed V_{BP} is obtained by the vector sum of $v_{\parallel}$ and $V_{sw\perp}$.

Figure 9. For the largest angle $\theta_{nB} = \theta_{max} = 65°$ at which the ions can escape upstream, the distribution peaks at $v_{\parallel} \simeq 500$ km/s with a parallel velocity spread $(v_{\parallel}^2 - \bar{v}_{\parallel}^2)^{1/2}$ of about 40 km/s when the angle between the solar wind and the interplanetary magnetic field ϕ_{vB} is 45° (Figure 9*a*). The perpendicular thermal spread for this case is about 95 km/s, that is, $T_{\perp}^{esc} \sim 50$ eV. Thus its perpendicular temperature is 5.5 times larger than the parallel temperature. As the angle θ_{nB} decreases, the distribution changes; the distribution, which is beamlike for $\theta_{nB} \sim 65°$, becomes oblate shaped for $\theta_{nB} \sim 55°$ with a perpendicular thermal spread of 160 km/s ($T_{\perp} \sim 130$ eV) and a maximum pitch angle of about 30°. The oblateness comes from the fact that the ions originate from two different source regions. One is close to the exit point, and the other is close to the perpendicular shock. The former forms a peak off the $v_{\parallel}$ axis in the distribution. When the angle ϕ_{vB} is changed from 45° to 67°, the parallel bulk speed increases as much as 15–30%. At the same time, the perpendicular temperature increases as much, but the parallel temperature does not change.

The flux of escaping ions calculated by the above model is shown in Figure 10. For model A, no ions escape above $\theta_{nB} = 55°$; this model, which uses the Rankine-Hugoniot relations, overestimates the bending of the field line at the shock surface because the global connection of the field lines is not taken into account. For model B with parallel field lines, the escaping ions first appear at $\theta_{nB} = 70°$, while for model C, which is a hybrid of models A and B, the ions first appear at $\theta_{nB} = 65°$. Thus the angle θ_{nB} at which the escaping ions first appear depends on the orientation of the field lines in the magnetosheath. The existence of this critical angle, $\theta_{nB} = \theta_{max}$, is due to the fact that the pitch-angle-scattered ions move with the convecting magnetic field and also that the ion source region is detached from the shock surface. Our calculated ion flux has a peak around $\theta_{nB} = 40°$–65° for model C, and its density is about 1.5% of the solar wind density (the flux density is about 2.5% of the solar wind flux), where we assumed that 10% of the incident solar wind ions become gyrating ions. For each case, the flux density decreases below the angle $\theta_{nB} \sim 45°$; however, this is due to the assumed decrease in the source ions as $\sin^2 \theta_{nB}$. If instead we use an ion source whose density is independent of the angle θ_{nB}, no qualitative change occurs in the ion density contours in the $(v_{\parallel}, v_{\perp})$ space. However, a fairly wide plateau of constant escaping flux density appears below $\theta_{nB} \lesssim 60°$, leading to a significant change in the flux density below 50° in Figure 10. If the pitch-angle-scattered ion source is switched off below a certain angle θ_c, then a plateau is formed for $\theta_c \lesssim \theta_{nB} \lesssim 65°$, and the escaping flux density decreases rapidly below θ_c. At present, we have little knowledge about the ion behavior at the shock with relatively small θ_{nB} angle (say, $\theta_{nB} \lesssim 60°$), and our results are increasingly unreliable for θ_{nB} smaller than 45°.

The largest angle θ_{max} for which ions, initially incident at the perpendicular shock ($\theta_{nB} = 90°$), can escape upstream can be determined in the following manner. As illustrated in Figure 8, we assume that the front one fourth of the bow shock may be approximated by a circle. We fix the x axis parallel to the interplanetary magnetic field and the y axis such that the coordinate of the perpendicular shock is $\mathbf{x}_0 = (0, R)$, where R is the radius of the magnetosheath. In this coordinate system the solar wind velocity is $\mathbf{V}_{sw} = (-V_{sw}/\sqrt{2}, -V_{sw}/\sqrt{2})$. After the ions crossed the point $\mathbf{X}_0$, they move at the downstream flow

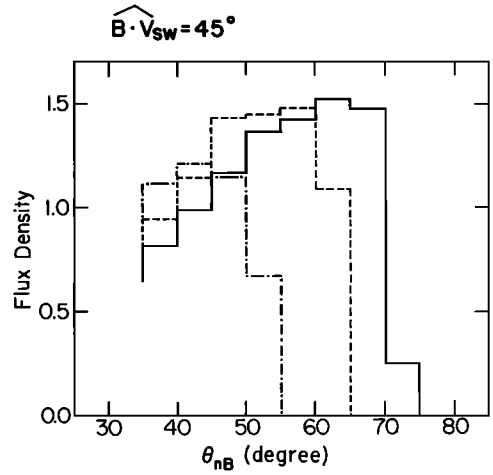

Fig. 10. Flux of escaping ions versus θ_{nB} for the case of $B \hat{} V_{sw} = \phi_{vB} = 45°$, where θ_{nB} is the angle between the shock normal and the interplanetary magnetic field **B**. Solid, dot-dash, and dashed lines correspond to calculations assuming model A, model B, and model C, respectively. Full scale in ordinate is about 3% of $n_1 V_{sw}$.

velocity $\mathbf{u}_2 = (-V_{sw}/\sqrt{2}, -\lambda V_{sw}/\sqrt{2})$, where $\lambda = B_1/B_2 \sim 0.3$ is assumed, and are then isotropized by EMIC instability as shown in section 2. Isotropization occurs at $\mathbf{x}_1$ ($\approx \mathbf{x}_0$); then ions move along the field line with the velocity $\mathbf{v} = \mathbf{u}_2 + v_{\parallel}e_x$ and reach the shock surface at $\mathbf{x}_2 = \mathbf{x}_1 + \mathbf{u}_2\tau$, where τ is the travel time and e_x is the unit vector in the x direction. By putting $|\mathbf{x}_2| = R$, we obtain $\tau V_{sw}/R \sim 2\sqrt{2}\lambda/(1 - \sqrt{2}\mu)^2$, where $\mu = v_{\parallel}/V_{sw}$. The angle θ_{max} of the escape point is thus

$$\tan \theta_{max} \sim (\sqrt{2}\mu - 1)/2\lambda$$

The angle θ_{max} is obtained by putting $\mu \sim \sqrt{2}$, yielding $\theta_{max} \sim 60°$. Ions with $\mu = v_{\parallel}/V_{sw} < \sqrt{2}$ reach the shock surface with a smaller escape angle (closer to the subsolar point).

4. DISCUSSION

In the preceding sections we have shown that backstreaming ion beams in the foreshock region are a natural consequence of the microscale and macroscale structure of the bow shock. An important and well-documented [*Montgomery et al.*, 1970; *Paschmann et al.*, 1982; *Leroy et al.*, 1982] macroscopic feature of the quasi-perpendicular portion of the bow shock is the reflection and energization of some of the incident ions at the magnetic ramp. These ions are magnetically deflected into the magnetosheath and phase mix to form a high-energy ring in velocity space. While convecting downstream, the ions are isotropized by microturbulent scattering due to the electromagnetic ion cyclotron instability. By this process some ions acquire large enough velocities parallel to the magnetic field to escape along field lines, which are connected to the upstream region due to the macroscale curvature of the shock surface.

This mechanism provides a natural explanation for the 'reflected' ion beams in the foreshock region with $\theta_{nB} \lesssim 65°$, roughly 95% of the observed cases [*Bonifazi and Moreno*, 1981*a*, *b*]. Without an additional acceleration mechanism, ions in our model cannot escape upstream for $\theta_{nB} \gtrsim 70°$ and thus cannot straightforwardly explain the remaining 5% of foreshock ion beams. There is likely to be some such acceleration, however, so that our model may also explain the ion beams with large θ_{nB}. This possibility is discussed in more detail later. We expect the results of our model to be quantitatively correct for $70° \gtrsim \theta_{nB} \gtrsim 45°$. For smaller θ_{nB}, the results are likely to be progressively more inaccurate, since the ion scattering process assumed is strictly valid only for the quasi-perpendicular bow shock. For oblique shocks, there are additional processes which can also lead to ions diverted back upstream. Some of the ions reflected at the shock front, which at the perpendicular shock must all eventually reach the downstream region, can at the oblique shock return directly into the upstream region [*Gosling et al.*, 1982]. These ions may in fact be related to the diffuse population. In addition, scattering of ions by the turbulent fields characteristic of oblique shocks can also increase the flux and the parallel temperature of the reflected ions. However, our model is likely to be qualitatively correct even for the foreshock beams with $\theta_{nB} \lesssim 45°$.

The characteristics of the ion beams produced in our model agree well with the observations, especially for $65° \gtrsim \theta_{nB} \gtrsim 45°$, for which the model is most accurate [*Gosling et al.*, 1978; *Bame et al.*, 1980; *Greenstadt et al.*, 1980; *Paschmann et al.*, 1981; *Bonifazi and Moreno*, 1981*a*, *b*]. The calculated density of the escaping ions n_{esc} is about 1–2% of the solar wind density n_{sw} for the parameters given in section 3. This value is in excellent agreement with the average observed relative density of about 1% [*Bonifazi and Moreno*, 1981*a*, *b*]. In our model the relative density of ions able to escape is proportional to the relative density of ions reflected at the magnetic ramp of the quasi-perpendicular shock which in turn is roughly proportional to the Alfven Mach number M_A [*Leroy et al.*, 1981]. *Paschmann et al.* [1981] appear to have failed to find significant correlation between the density of reflected ions and M_A in an analysis of a small number of cases (20). This correlation could be difficult to measure experimentally. The relevant Mach number M_A is based on the solar wind velocity component normal to the shock where the ions initially cross the shock. Observationally, only the local conditions at the spacecraft are known. Using the observed ion beam velocity, the point where the beam leaves the shock can be inferred. In our model, ions after being scattered recross the shock and flow upstream at significantly smaller θ_{nB}. It is further necessary to average the local M_A at the various sections that contribute to the ions observed at some point upstream, which would smear out the correlation.

The calculated ion density decreases below $\theta_{nB} \sim 45°$ (Figure 10); however, the decrease is based on the assumption that ions are mainly supplied by the quasi-perpendicular shock (source density $\propto \sin^2 \theta_{nB}$) which is increasingly questionable for small θ_{nB}. The assumption of a constant source density gives a wide plateau below $\theta_{nB} \sim 60°$, as mentioned in section 3.

The parallel velocity of the calculated escaping ions in the shock frame ranges from $v_{\parallel}/V_{sw} \sim 1.4$ (1.5) at $\theta_{nB} = 65°$ to $v_{\parallel}/V_{sw} \sim 1.7$ (1.8) at $\theta_{nB} = 45°$ for the case where the angle between the solar wind and the interplanetary magnetic field ϕ_{vB} is 45° (67°). Then the total bulk velocity in the foreshock region V_{BF}/V_{sw} becomes 1.5 (1.9) at $\theta_{nB} = 65°$ and 1.8 (2.0) at $\theta_{nB} = 45°$. These results are rather independent of M_A, since the ratio of the gyrating ion velocity to solar wind velocity V_{sw} is roughly constant [*Leroy et al.*, 1982]. Our results are consistent with the observed average value of the backstreaming bulk velocity of the reflected ions, about $2.0V_{sw}$, which is only very weakly dependent on θ_{nB} (for $\theta_{nB} < 65°$) [*Bonifazi and Moreno*, 1981*a*, *b*]. The calculated upstream velocity, however, depends on the angle between the solar wind and the interplanetary magnetic field. The present calculations assumed this angle is 45° and 67°. When this angle is increased, so that there is less incident parallel velocity, the scattered ions expend less energy in turning around to come back upstream and thus escape with larger energies.

The values of V_{BF}/V_{sw} calculated from our model appear also to be consistent with the upstream ion events discussed in the work of *Paschmann et al.* [1980]. We note, however, that our results are significantly smaller than those predicted by the geometric energization formulas of *Sonnerup* [1969] and *Paschmann et al.* [1980], assuming μ to be conserved. Although the data of *Paschmann et al.* [1980] generally agree with these predictions, there is considerable scatter. For $45° < \theta_{nB} < 65°$ (which, using our model parameters, corresponds to $5 \lesssim (E_r/E_i)_{th} \lesssim 15$ in Figure 2 of *Paschmann et al.* [1980]), there are several events for which $(E_r/E_i)_{obs} = V_{BF}^2/V_{sw}^2$ is approximately 4. These observations agree both with our results and with those of *Bonifazi and Moreno* [1981*a*, *b*].

Paschmann et al. [1980] also found ion events with beam speed well above the speeds we can straightforwardly produce in our model for $\theta_{nB} \gtrsim 45°$. This subset of their data agrees very well with the geometric energization formulas of *Sonnerup* [1969] and *Paschmann et al.* [1980]. These high-energy beams may, in fact, be a separate population of ions that are directly reflected upstream at the shock.

Higher-energy beams can also be produced by a plausible extension of our model. We can assume that in addition to

TABLE 1. Summary of Model Calculations Presented in This Paper With Observations of ISEE Satellites

	Model	Observation
Detection region, θ_{nB}	$\lesssim 65°$	$\lesssim 70°$*†
Density, n_{esc}/n_{sw}	1–2%	1%†
Bulk speed, V_{BP}/V_{sw}	1.5–2.0	2.0†
Temperature anisotropy, $T_\perp/T_\parallel$	3–5‡	2–3*

θ_{nB} is the angle between the shock normal and the upstream magnetic field at which ions first escape.
*Paschmann et al. [1981].
†Bonifazi and Moreno [1981a, b].
‡Warm ring with ±20% spread.

being pitch angle scattered, the gyrating ions downstream of the shock are thermalized by electrostatic turbulence. This thermalization, though not the primary agent, is evident observationally [*Paschmann et al.*, 1982]. The gyrating ions would be heated by the turbulence producing some more energetic ions. The calculations of *Kulygin et al.* [1971] clearly show that the interaction of a cold ring with energy ε_0 with the ambient plasma generates a thermal spread around ε_0 of the order $\Delta\varepsilon = 0.5\varepsilon_0$, with ions reaching energies up to $2.3\varepsilon_0$ (see Figure 1 of *Kulygin et al.* [1971]). The net effect would probably be to produce higher-energy beams for large θ_{nB} ($\gtrsim 70°$) rather than increase the beam speed for moderate θ_{nB}. We can invert the argument used in section 3 to determine the exit angle of an ion as a function of velocity to obtain

$$\frac{V_{BP}}{V_{sw}} \equiv \left(\frac{E_r}{E_i}\right)^{1/2} = \frac{1}{\sqrt{2}}\left[\left(1 + 2\frac{B_1}{B_2}\tan\theta_{nB}\right)^2 + 1\right]^{1/2}$$

Assuming this relation to hold for $\theta_{nB} > 70°$, we find that V_{BP}/V_{sw} is 2.4 for $\theta_{nB} = 75°$ and 3.2 for $\theta_{nB} = 80°$. These results agree very well with findings of *Bonifazi and Moreno* [1981a, b]. The values calculated for the two events with θ_{nB} slightly greater than 70° by *Paschmann et al.* [1980] are significantly higher, ~5, which are consistent with *Sonnerup* [1969].

The distributions of escaping ions in section 3 show the large temperature anisotropy inherent in our model. This is an important result as this anisotropy is a universal characteristic of the 'reflected' ion beams [*Paschmann et al.*, 1981], which is difficult to explain in the context of the direct reflection model. The model anisotropy is somewhat larger than observed $T_\perp/T_\parallel \sim 6$ for $\theta_{nB} = 65°$ ($\phi_{vB} = 45°$). Furthermore, some of the distributions shown in Figure 9 are peaked at $v_\perp \neq 0$ and hence are loss-cone-like instead of monotonic in velocity, as is usually observed. These distributions should, however, be considered as upper limits, since we have neglected effects that would tend to make them more isotropic. We have also assumed that the ring ions had negligible thermal spread. The anisotropy is relaxed by introducing a reasonable thermal spread to the source ions. When the thermal spread Δv is included such that $|v| = [v_\perp{}^2 + (v_\parallel - v_\phi - u_\parallel)^2]^{1/2} \sim v_0 \pm \Delta v$, with $v_0 \sim 500$ km/s, $\Delta v/v_0 = 0.2$, then the parallel thermal width of the escaping ions becomes larger and the temperature anisotropy is reduced to 2.9 for $\theta_{nB} = 65°$, and 4.0 for $\theta_{nB} = 50°$. The ring thermal spread, and thus the beam parallel temperature, would be increased further because of the interaction of the core and ring ions due to electrostatic turbulence [*Kulygin et al.*, 1971; *Lee and Birdsall*, 1979a, b]. We have also assumed that the pitch angle scattering due to EMIC waves results only in isotropization of the rings ions; we neglect any scattering of ions in the magnetosheath as they move toward the shock surface. Finally, we note that the 'reflected' ion beams are usually observed some distance from the bow shock, so that further relaxation of the distribution is possible. Thus the somewhat smaller observed temperature anisotropy $T_\perp/T_\parallel = 2$–3 [*Paschmann et al.*, 1981] is consistent with our results. A summary of the results obtained by the calculations of section 3 is shown in Table 1, contrasted with the corresponding ISEE observations for $\theta_{nB} \lesssim 70°$.

In addition to the observed reflected beams, there are other observational data from the bow shock supporting our model. We consider first the downstream wave measurements. The ISEE 2 magnetic field data of November 7, 1977, show low-frequency magnetic field oscillations in the component perpendicular to the ambient magnetic field, which start a minute behind the shock transition and are observed for more than a few minutes in the downstream region (J. D. Scudder et al., unpublished manuscript, 1982). The frequency of these oscillations in the spacecraft frame is 0.2–0.3 Hz, and their amplitude is about 5 γ. This frequency corresponds to the ion cyclotron frequency ($f_{ci} \sim 0.3$ Hz), which is roughly the frequency of the EMIC waves. (In general, the frequency measured near the quasi-perpendicular shock may be Doppler shifted by as much as 100%, since the wave vectors of the EMIC waves satisfy $ck/\omega_{pi} \sim 1$ and the ion beta is close to unity, that is $\Delta\omega_D/\omega_{ci} = \mathbf{k}\cdot\mathbf{v}_\parallel/\omega_{ci} \lesssim \sqrt{\beta_i}\, v_\parallel/v_{ti} \sim 1$.) According to the saturation level observed in the simulations, the amplitude of the EMIC waves is estimated to be 10 γ, where we used $\delta B^2/8\pi n\langle T_i\rangle \sim 4 \times 10^{-2}$, $n = 40$ cm^{-3} and $\langle T_i\rangle \sim 150$ eV. The calculated value is a little higher than that observed; however, the former should be understood as the maximum in a one-dimensional k spectrum.

The positive ion measurements of *Gurgiolo et al.* [1981] further support our model. The Berkeley-Toulouse-Washington (BTW) fixed voltage electrostatic analyzer points in the GSE southward direction with narrow angular acceptance and thus detects northward moving positive ions with energies above 1.3 keV [*Anderson et al.*, 1978]. During the November 7, 1977, bow shock crossing of ISEE 1 and 2, the results of *Gurgiolo et al.* [1981] show little or no ion flux increase at the magnetic ramp but a large enhancement in observed flux roughly 1 min later in each case, that is, about at the same point as the low-frequency waves discussed above. We interpret these results as evidence of the EMIC wave-induced pitch angle scattering of the gyrating ions. For these events the interplanetary magnetic field was inclined roughly 45° to the ecliptic plane. The gyrating ions form fairly narrow beams in the plane perpendicular to **B** and, although sufficiently energetic, would not be detected by the BTW instrument. As the ions are scattered, some enter the detection window of the instrument, causing the flux enhancement. Owing to the inclination of **B** with respect to the instrument normal, this occurs before full isotropization is achieved.

In summary, we find that at least a substantial fraction of the 'reflected' ion beams observed in the foreshock region are likely to originate in the magnetosheath downstream of the quasi-perpendicular bow shock. These beams are a natural and necessary consequence of the observationally and theoretically well documented characteristics of this region of the bow shock. Our model reproduces well the average observed energy, temperature, and thermal anisotropy of the upstream beams for $\theta_{nB} \lesssim 65°$, and can be plausibly extended to produce higher-energy beams observed for $\theta_{nB} \gtrsim 70°$. Furthermore, there is observational evidence in the downstream region supporting the existence of the EMIC turbulence and associated ion pitch

angle scattering postulated in our model. Our model cannot easily explain the more energetic subset of the ion beams studied by *Paschmann et al.* [1980], which may indicate that direct reflection also produces some upstream ions.

Acknowledgments. We are grateful to C. S. Wu and M. M. Leroy for valuable comments and discussions, especially about the results of the hybrid simulations. We are also grateful to J. D. Scudder and A. Mangeney regarding ISEE data prior to publication. This work was supported by the NASA Solar Terrestrial Theory Program NAGW-81 and partially by ONR N00014-79-C-0665.

REFERENCES

Anderson, K. A., R. P. Lin, R. J. Paoli, G. K. Parks, C. S. Lin, H. Reme, J. M. Bosqued, F. Martel, F. Cotin, and A. Cros. An experiment to study energetic particle fluxes in and beyond the earth's outer magnetosphere, *IEEE Trans. Geosci. Electron., GE-16*, 213, 1978.

Asbridge, J. R., S. J. Bame, and I. B. Strong, Outward flow of protons from the earth's bow shock, *J. Geophys. Res., 73*, 5777, 1968.

Bame, S. J., J. R. Asbridge, W. C. Feldman, J. T. Gosling, G. Paschmann, and N. Sckopke, Deceleration of the solar wind upstream from the earth's bow shock and the origin of diffuse upstream ions, *J. Geophys. Res., 85*, 2981, 1980.

Bonifazi, C., and G. Moreno, Reflected and diffuse ions backstreaming from the earth's bow shock, 1, Basic properties, *J. Geophys. Res., 86*, 4397, 1981*a*.

Bonifazi, C., and G. Moreno, Reflected and diffuse ions backstreaming from the earth's bow shock, 2, Origin, *J. Geophys. Res., 86*, 4405, 1981*b*.

Busnardo-Neto, J., P. L. Pritchett, A. T. Lin, and J. M. Dawson, A self-consistent magnetostatic particle code for numerical simulation of plasmas, *J. Comp. Phys., 23*, 300, 1977.

Davidson, R. C., and J. M. Ogden, Electromagnetic ion cyclotron instability driven by ion energy anisotropy in high-beta plasmas, *Phys. Fluids, 18*, 1045, 1975.

Edmiston, J. P., C. F. Kennel, and D. Eichler, Escape of heated ions upstream of a quasi-parallel shock, *Geophys. Res. Lett., 9*, 531, 1982.

Gosling, J. T., J. R. Asbridge, S. J. Bame, G. Paschmann, and N. Sckopke, Observations of two distinct populations of bow shock ions in the upstream solar wind, *Geophys. Res. Lett., 5*, 957, 1978.

Gosling, J. T., M. F. Thomsen, S. J. Bame, W. C. Feldman, G. Paschmann, and N. Sckopke, Evidence for specularly reflected ions upstream from the quasi-parallel bow shock, *Geophys. Res. Lett.*, in press, 1982.

Greenstadt, E. W., The upstream escape of energized solar wind protons from the bow shock, in *The Magnetospheres of the Earth and Jupiter*, edited by V. Formisano, p. 3, D. Reidel, Hingham, Mass., 1975.

Greenstadt, E. W., C. T. Russel, and M. Hoppe, Magnetic field orientation and suprathermal ion streams in the earth's foreshock, *J. Geophys. Res., 85*, 3473, 1980.

Gurgiolo, C., G. K. Parks, B. H. Mauk, S. C. Lin, K. A. Anderson, R. P. Lin, and H. Reme, Non-$E \times B$ ordered ion beams upstream of the earth's bow shock, *J. Geophys. Res., 86*, 4415, 1981.

Kennel, C. F., and M. F. Engelmann, Velocity space diffusion from weak plasma turbulence in a magnetic field, *Phys. Fluids, 9*, 2377, 1966.

Kulygin, V. M., A. B. Mikhailovskii, and E. S. Tsapelkin, Quasi-linear relaxation of fast ions moving transverse to a magnetic field, *Plasma Phys., 13*, 1111, 1971.

Lee, J. K., and C. K. Birdsall, Velocity space ring-plasma instability, magnetized, I, Theory, *Phys. Fluids, 22*, 1306, 1979*a*.

Lee, J. K., and C. K. Birdsall, Velocity space ring-plasma instability, magnetized, II, Simulation, *22*, 1315, 1979*b*.

Lee, K., J. U. Brackbill, D. W. Forslund, and K. Quest, Dissipation of reflected ion beams from quasi-perpendicular shocks due to electromagnetic ion cyclotron instability (abstract), *Eos Trans. AGU, 62*, 1011, 1981.

Leroy, M. M., C. C. Goodrich, D. Winske, C. S. Wu, and K. Papadopoulos, Simulation of a perpendicular bow shock, *Geophys. Res. Lett., 8*, 1269, 1981.

Leroy, M. M., D. Winske, C. C. Goodrich, C. S. Wu, and K. Papadopoulos, The structure of perpendicular bow shock, *J. Geophys. Res., 87*, 5081, 1982.

Lin, R. P., C.-I. Meng, and K. A. Anderson, 30- to 100-keV protons upstream from the earth's bow shock, *J. Geophys. Res., 79*, 489, 1974.

Montgomery, M. D., J. R. Asbridge, and S. J. Bame, Vela 4 plasma observations near the earth's bow shock, *J. Geophys. Res., 75*, 1217, 1970.

Paschmann, G., N. Sckopke, J. R. Asbridge, S. J. Bame, and J. T. Gosling, Energization of solar wind ions by reflection from the earth's bow shock, *J. Geophys. Res., 85*, 4689, 1980.

Paschmann, G., N. Sckopke, I. Papamastorakis, J. R. Asbridge, S. J. Bame, and J. T. Gosling, Characteristics of reflected and diffuse ions upstream from the earth's bow shock, *J. Geophys. Res., 86*, 4355, 1981.

Paschmann, G., N. Sckopke, S. J. Bame, and J. T. Gosling, Observations of gyrating ions in the foot of the nearly perpendicular bow shock, *Geophys. Res. Lett., 9*, 881, 1982.

Sonnerup, B. U. O., Acceleration of particles reflected at a shock front, *J. Geophys. Res., 74*, 1301, 1969.

Tajima, T., K. Mima, and J. M. Dawson, Alfven ion cyclotron instability: Its physical mechanism and observation in computer simulation, *Phys. Rev. Lett., 39*, 201, 1977.

Terasawa, T., Energy spectrum and pitch angle distribution of particles reflected by MHD shock waves of fast mode, *Planet. Space Sci., 27*, 193, 1979.

Tidman, D. A., and N. A. Krall, *Shock Waves in Collisionless Plasmas*, Interscience, New York, 1971.

Wu, C. S., Physical mechanisms for turbulent dissipation in collisionless shock waves, *Space Sci. Rev., 32*, 83, 1982.

(Received August 3, 1982;
revised January 24, 1983;
accepted January 26, 1983.)